Equilibration of right-handed electrons

Dietrich Bödeker and Dennis Schröder

Fakultät für Physik, Universität Bielefeld,
33501 Bielefeld, Germany

E-mail: bodeker@physik.uni-bielefeld.de, dennis@physik.uni-bielefeld.de

Abstract. We study the equilibration of right-handed electrons in the symmetric phase of the Standard Model. Due to the smallness of the electron Yukawa coupling, it happens relatively late in the history of the Universe. We compute the equilibration rate at leading order in the Standard Model couplings, by including gauge interactions, the top Yukawa- and the Higgs self-interaction. The dominant contribution is due to $2 \to 2$ particle scattering, even though the rate of (inverse) Higgs decays is strongly enhanced by multiple soft scattering which is included by Landau-Pomeranchuk-Migdal (LPM) resummation. Our numerical result is substantially larger than approximations presented in previous literature.

Contents

1 Introduction

The electron Yukawa coupling is the smallest coupling constant of the Standard Model. Therefore thermal equilibrium between right- and left-handed electrons is achieved relatively late in the evolution of the Universe. Nevertheless, it happened in the symmetric phase, while electroweak sphaleron processes were still rapidly violating baryon plus lepton number. Therefore the equilibration of right-handed electrons can play an important role in the creation of the matter- antimatter-asymmetry of the Universe.

A matter-antimatter asymmetry created at some very high temperature like, e.g. in GUT baryogenesis, can be protected from washout if the right-handed electrons [1, 2] are not yet in equilibrium. Baryogenesis through neutrino oscillations [3, 4], for certain model parameters, can take place at the same time as the equilibration of the right-handed electrons. Then the latter is part of the leptogenesis process. A lepton asymmetry in right-handed electrons may also generate hypermagnetic fields [5].

The importance of electron equilibration was first pointed out in [1], where it was noted that the final baryon asymmetry is exponentially sensitive to the equilibration rate. A

computation in [1] included only the inverse Higgs decay. The importance of $2 \to 2$ scattering was noted in [2]. The equilibration of heavier lepton flavors in thermal leptogenesis was studied in [6, 7]. It was pointed out that multiple soft $1n \leftrightarrow 2n$ scattering processes also contribute at leading order [7], and the corresponding rate was estimated, but it has not been computed so far.

In this paper we only consider the equilibration rate of right-handed electrons $e_{\rm R}$. We improve on previous calculations by correctly treating various thermal effects. Furthermore, for the first time, we compute the contributions from multiple soft gauge interactions in collinear emission processes. We consider temperatures T well below $10^{14}\,{\rm GeV}$. Then weak hypercharge interactions are much faster than the Hubble expansion, and the right-handed electrons are in kinetic equilibrium. Due to the smallness of the electron Yukawa coupling the lepton number $L_{e\rm R}$ carried by $e_{\rm R}$ takes much longer to equilibrate. For sufficiently small deviations from equilibrium the time evolution of $L_{e\rm R}$ can be described by a linear equation. Without Hubble expansion it can be written as

$$\dot{L}_{e\rm R} = -\gamma \left(L_{e\rm R} - L_{e\rm R}^{\rm eq} \right) + \cdots . \tag{1.1}$$

There may by additional contributions on the right-hand side due to other slowly varying charges. Furthermore, the chiral anomaly violates $L_{e\rm R}$-conservation in the Standard Model. Therefore $L_{e\rm R}$ can be converted into hypercharge electromagnetic fields, changing the value of $L_{e\rm R}$. In the absence of long-range gauge fields this is a non-linear effect. However, complete equilibration may in fact lead to long-range hypermagnetic fields [8]. These effects can be neglected as long as the growth rate of the gauge fields is smaller than γ in (1.1). In the Standard Model this requires that the chemical potential conjugate to $L_{e\rm R}$ satisfies (see appendix D)

$$|\mu_{L_{e\rm R}}| \lesssim 1.4 \cdot 10^{-3} T \tag{1.2}$$

when γ is comparable to the Hubble rate.

The processes contributing to the rate γ are very similar to those in the production of ultrarelativistic sterile neutrinos [9, 10]. There are two different types of contributions at leading order, which is $h_e^2 g^2$ where g denotes a generic Standard Model coupling and h_e is the electron Yukawa coupling. The first type are $2 \to 2$ scattering processes. The second includes the (inverse) $1 \leftrightarrow 2$ decay of Higgs bosons into right-handed electrons and lepton doublets. This decay is kinematically allowed when the thermal Higgs mass is sufficiently large. One also has to take into account $1n \leftrightarrow 2n$ scatterings with soft gauge boson exchanges. Due to their collinear nature these processes are not suppressed. On the contrary, they lead to strong enhancement compared to the rate for Higgs decay, because they open several new channels, which also happens in sterile neutrino production [10]. Therefore the multiple scatterings of $1n \leftrightarrow 2n$ particles with arbitrary n have to be included, which is known as Landau-Pomeranchuk-Migdal (LPM) resummation [11–13]. A complication compared to sterile neutrino production is that right-handed electrons have Standard Model gauge interactions, because they carry weak hypercharge. Therefore they are also affected by multiple scattering, similar to gluons in QCD [14–16].

In section 2 we recall general expressions for equilibration rates, and apply them to $e_{\rm R}$ equilibration. In section 3 we compute the contribution from (inverse) Higgs decays and $1n \leftrightarrow 2n$ processes. The $2 \to 2$ processes are treated in section 4. Section 5 contains numerical results and comparison with previous work. Susceptibilities are computed in appendix A.

The solution to the integral equation which sums all $1n \leftrightarrow 2n$ processes is described in appendix B, and some integrals for the $2 \to 2$ processes are treated in appendix C. We estimate the conversion of L_{eR} into hypermagnetic fields through the chiral anomaly and obtain the bound (1.2) in appendix D.

Notation and conventions. We write four-vectors in lower-case italics, k, and the corresponding three-vectors in boldface, $\mathbf{k}$. Integrals over three-momentum are denoted by $\int_{\mathbf{k}} \equiv (2\pi)^{-3} \int d^3 k$. When working in imaginary time we have four-vectors $k = (k^0, \mathbf{k})$ with $k^0 = \pi i n T$ with n even (odd) for bosons (fermions). We denote fermionic Matsubara sums by a tilde, $\widetilde{\sum}_{k^0}$. We use the metric with signature $(+, -, -, -)$. Covariant derivatives are $D_\mu = \partial_\mu + i y_\alpha g' B_\mu + \cdots$ with the hypercharge gauge coupling g' and gauge field B, such that $y_\varphi = 1/2$ for the Higgs field φ. The quartic term in the Higgs potential is $\lambda(\varphi^\dagger \varphi)^2$.

2 Equilibration rates from thermal field theory

2.1 General considerations

We consider one or several charges Q_a which are almost conserved, meaning that they change much more slowly than most other ("fast") degrees of freedom in the hot plasma. The fast degrees of freedom equilibrate on a much shorter time scale than the slow ones. We are interested in the long time behavior, that is on the time evolution of the slow variables, so that the fast ones are always in equilibrium. We assume small deviations $\delta Q_a \equiv Q_a - Q_a^{\mathrm{eq}}$ from thermal equilibrium, so that the time evolution of δQ_a is determined by linear equations.[1] Without the Hubble expansion these effective kinetic equations are of the form

$$\dot{Q}_a = -\gamma_{ab} \delta Q_b. \tag{2.1}$$

Both Q_a^{eq}, and the rates γ_{ab} only depend on the temperature of the fast degrees of freedom, and of the values of the strictly conserved charges. The rates can be written as [17, 18][2]

$$\gamma_{ab} = \frac{1}{V} \lim_{\omega \to 0} \frac{1}{\omega} \mathrm{Im} \Pi_{ac}^{\mathrm{ret}}(\omega) \left(\Xi^{-1} \right)_{cb} \tag{2.2}$$

where V is the volume, which will be taken to infinity, and

$$\Pi_{ab}^{\mathrm{ret}}(\omega) \equiv i \int_0^\infty dt \, e^{i\omega t} \left\langle \left[\dot{Q}_a(t), \dot{Q}_b(0) \right] \right\rangle \tag{2.3}$$

is a retarded correlation function, which is computed in thermal equilibrium. The matrix of susceptibilities Ξ is determined by the fluctuations of δQ_a in thermal equilibrium,

$$\Xi_{ab} \equiv \frac{1}{TV} \langle \delta Q_a \delta Q_b \rangle, \tag{2.4}$$

taken at fixed values of strictly conserved charges.

At leading order in the Q_a-violating interaction strength one can neglect these interactions in the expectation values in (2.3) and (2.4), so that the Q_a violation appears only in

---

[1] In [17, 18] the conserved charges and the equilibrium values of the slow charges are assumed to vanish. Here we allow for non-zero values for both of them.

[2] We assume that the operators Q_a commute at equal times.

the operators $\dot{Q}_a$ in (2.3). Then one can introduce chemical potentials μ_a for the Q_a. For the charge densities $n_a \equiv Q_a/V$ we have at linear order

$$\delta n_a = \Xi_{ab}\mu_b. \tag{2.5}$$

Thus the kinetic equations (2.1) are equivalent to

$$\dot{n}_a = -\Gamma_{ab}\mu_b, \tag{2.6}$$

with

$$\Gamma_{ab} = \frac{1}{V}\lim_{\omega\to 0}\frac{1}{\omega}\mathrm{Im}\Pi_{ab}^{\mathrm{ret}}(\omega). \tag{2.7}$$

The coefficients Γ_{ab} are functions of the temperature and of the values of strictly conserved charges.

The equations (2.6) for n_a can be closed as follows. One introduces chemical potentials not only for the slowly varying charges but also for the strictly conserved ones. One computes the pressure P as a function of these chemical potentials. Then the charge densities are given by

$$n_A = \frac{\partial P}{\partial \mu_A}, \tag{2.8}$$

where upper case indices label both slowly violated and strictly conserved charges. These are relations between all charge densities and all chemical potentials. They can be solved to give the chemical potentials of the slowly varying charges in terms of all charge densities.

We assume all charge densities to vanish for zero chemical potentials. If the charge densities are sufficiently small, the required relations are

$$n_A = \chi_{AB}\mu_B \tag{2.9}$$

with the matrix of susceptibilities

$$\chi_{AB} \equiv \left.\frac{\partial^2 P}{\partial \mu_A \partial \mu_B}\right|_{\mu=0}. \tag{2.10}$$

2.2 Right-handed electrons

Let us now apply the above formulas to the equilibration of right-handed electrons. In the Standard Model the lepton number

$$L_{e\mathrm{R}} \equiv \int d^3x\, e_{\mathrm{R}}^\dagger e_{\mathrm{R}} \tag{2.11}$$

carried by right-handed electrons is violated by their Yukawa interaction

$$\mathscr{L}_{\mathrm{int}} = -h_e \overline{e_{\mathrm{R}}}\varphi^\dagger \ell + \mathrm{H.c.} \tag{2.12}$$

with the Higgs field φ and the left-handed electron doublet ℓ. The electron Yukawa coupling h_e is chosen to be real. $L_{e\mathrm{R}}$ is also violated by the chiral anomaly which can lead to the creation of hypercharge magnetic fields [5].

The time derivative of L_{eR} due to the Yukawa interaction (2.11) reads

$$\dot{L}_{eR} = -i \int d^3x \left(h_e \overline{e_R} \varphi^\dagger \ell - \text{H.c.} \right).$$ (2.13)

This will be used to compute

$$\Gamma \equiv \Gamma_{L_{eR} L_{eR}},$$ (2.14)

by means of (2.3), (2.7). The chiral anomaly term does not contribute to (2.7), since the hypercharge gauge field is abelian, and unlike in non-abelian gauge theories the corresponding winding number does not diffuse.

To determine the chemical potentials on the right-hand side of (2.7), we have to identify the strictly conserved charges and determine their correlations. In the symmetric phase, the conservation of baryon number B and the lepton numbers L_α in flavor α are violated by electroweak sphalerons. However, in the Standard Model the charges

$$X_\alpha \equiv L_\alpha - \frac{B}{3}$$ (2.15)

are conserved. Furthermore, gauge charges are conserved. In the symmetric phase the non-abelian gauge charges are not correlated with the weak hypercharge Y or with non-gauge charges. However, the correlation of L_{eR} with the weak hypercharge does not vanish, $\chi_{L_{eR}Y} \neq 0$, and must be included in (2.9). In the imaginary time formalism the temporal component of the hypercharge gauge field B_0 is purely imaginary. It has a non-zero expectation value [19], which plays the role of a hypercharge chemical potential,

$$\mu_Y = i g' B_0,$$ (2.16)

ensuring hypercharge neutrality.

To illustrate the use of (2.6) and (2.9) consider three important examples. We need the inverse of the susceptibility matrix χ, which is computed in appendix A.

1. Only Standard Model interactions, L_{eR} is the only slow variable. Assume X_e to be non-zero, and $X_\mu = X_\tau = 0$. Then (2.9) gives

$$\mu_{L_{eR}} = \left(\chi^{-1} \right)_{L_{eR} L_{eR}} n_{L_{eR}} + \left(\chi^{-1} \right)_{L_{eR} X_e} n_{X_e},$$ (2.17)

which we write as

$$\mu_{L_{eR}} = \left(\chi^{-1} \right)_{L_{eR} L_{eR}} \left(n_{L_{eR}} - n_{L_{eR}}^{\text{eq}} \right)$$ (2.18)

with

$$n_{L_{eR}}^{\text{eq}} = - \frac{\left(\chi^{-1} \right)_{L_{eR} X_e}}{\left(\chi^{-1} \right)_{L_{eR} L_{eR}}} n_{X_e}$$ (2.19)

Combining this with (2.6) yields

$$\dot{n}_{L_{eR}} = -\gamma \left(n_{L_{eR}} - n_{L_{eR}}^{\text{eq}} \right)$$ (2.20)

with

$$\gamma = \left(\chi^{-1}\right)_{L_{eR}L_{eR}} \Gamma. \tag{2.21}$$

Equation (A.2) then gives

$$\gamma = \frac{4266}{481} T^{-2}\Gamma, \tag{2.22}$$

$$n_{L_{eR}}^{\mathrm{eq}} = \frac{185}{711} n_{X_e}. \tag{2.23}$$

2. Only Standard Model interactions, L_{eR} is the only slow variable. Now allow for all X_α to be non-vanishing, with the constraint $B - L = \sum_\alpha X_\alpha = 0$. Then we have

$$\dot{n}_{L_{eR}} = -\Gamma \left[\left(\chi^{-1}\right)_{L_{eR}L_{eR}} n_{L_{eR}} + \sum_\alpha \left(\chi^{-1}\right)_{L_{eR}X_\alpha} n_{X_\alpha} \right]. \tag{2.24}$$

By means of (A.2) this turns into

$$\dot{n}_{L_{eR}} = -T^{-2}\Gamma \left[\frac{4266}{481} n_{L_{eR}} - \frac{30}{13} n_{X_e} + \frac{24}{37} \left(n_{X_\mu} + n_{X_\tau} \right) \right]. \tag{2.25}$$

This equation can be recast in the form of (2.20) with (2.22) and

$$n_{L_{eR}}^{\mathrm{eq}} = \frac{1}{3} n_{X_e}, \tag{2.26}$$

which agrees with the result in [2].

3. Type-I see-saw models realizing leptogenesis. Here one supplements the Standard Model with right-handed Majorana neutrinos whose Yukawa interactions violate X_α-conservation. If leptogenesis takes place around the same time as the equilibration of right-handed electrons, then both the X_α and L_{eR} have to be treated as slow variables. The time derivatives of X_α are uncorrelated with (2.13), and therefore the rate coefficients $\Gamma_{L_{eR}X_\alpha}$ vanish. In this case (2.24) and (2.25) hold again, and so does (2.22). This time the terms with n_{X_α} do not contribute to $n_{L_{eR}}^{\mathrm{eq}}$, but constitute individual source terms, so that $n_{L_{eR}}^{\mathrm{eq}} = 0$ and

$$\gamma_{L_{eR}X_e} = -\frac{30}{13} T^{-2}\Gamma, \tag{2.27}$$

$$\gamma_{L_{eR}X_\alpha} = \frac{24}{37} T^{-2}\Gamma \qquad (\alpha = \mu, \tau). \tag{2.28}$$

We evaluate Γ at vanishing chemical potentials, which is appropriate when the charge densities are small. This way we avoid the problem of infrared divergences in processes with Higgs bosons in the initial or final state (see [20]).

Figure 1. The interference of these two exemplary $1n \to 2n$ processes with $n = 2$ needs to be taken into account. The gauge bosons have soft momenta $q \sim gT$.

3   Higgs decay and multiple soft scattering

The bulk of particles in the plasma have 'hard' momenta, $p \sim T$. In the symmetric phase, the Standard Model particles carry thermal masses. For the Higgs boson the thermal mass is momentum independent and is given by [21]

$$m_\varphi^2 = \frac{1}{16} \left[3g^2 + g'^2 + 4h_t^2 + 8\lambda \right] (T^2 - T_0^2), \tag{3.1}$$

with $T_0 = 160\,\mathrm{GeV}$. For hard fermions one has to use the so-called asymptotic thermal masses [21], which for the left- and right-handed leptons are given by[3]

$$m_\ell^2 = \frac{1}{16} \left[3g^2 + g'^2 \right] T^2, \tag{3.2}$$

$$m_{e_\mathrm{R}}^2 = \frac{1}{4} g'^2 T^2. \tag{3.3}$$

For $T \gg T_0$ the Higgs bosons have the largest mass, and for certain values of the couplings their decay into left-handed lepton doublets ℓ and the right-handed electrons is kinematically allowed. With increasing temperature the top Yukawa coupling decreases such that above a certain temperature m_φ becomes smaller than $m_\ell + m_{e_\mathrm{R}}$ and the channel closes. Since $m_\varphi > m_\ell > m_{e_\mathrm{R}}$ at any temperature well above the electroweak scale, no other $1 \leftrightarrow 2$ decay channel opens up at a higher temperature.

Since the masses are small compared to T, the particles participating in the decay process are ultrarelativistic. Furthermore, their momenta are nearly collinear, with transverse momenta $p_\perp$ of order gT. The wave packets of the decay products have a width of order $1/p_\perp$. They overlap for a time of order $1/(g^2 T)$, the so-called formation time. Here the formation time is of the same order of magnitude as the mean free time between scatterings with 'soft' momentum transfer $q \sim gT$. Thus the particles typically scatter multiple times before their wave packets separate, so that the scatterings cannot be treated independently. We show two exemplary diagrams in figure 1. This situation is similar to bremsstrahlung in a medium in QED [11–13, 22] (see also [23]), and in QCD [14–16, 24, 25], where it leads to a suppression of the emission probability. In the case of sterile neutrino production, on the other hand, it gives a strong enhancement, because new kinematic channels are opened [10]. We compute the Higgs decay in section 3.1, and include multiple soft scatterings in section 3.2.

---

[3]For fermions the asymptotic mass is a factor $\sqrt{2}$ larger than the one at zero momentum [21]. In [2] the zero-momentum fermion masses are used.

3.1 Higgs decay

We start from the imaginary-time correlator

$$\Pi_{L_{eR}L_{eR}}(i\omega_n) = \int\limits_0^{1/T} d\tau\, e^{i\omega_n\tau} \langle \dot{L}_{eR}(-i\tau)\dot{L}_{eR}(0)\rangle, \tag{3.4}$$

with bosonic frequency ω_n. Without soft gauge interactions, (3.4) reads

$$\Pi_{L_{eR}L_{eR}}(i\omega_n) = -2V h_e^2 T^2 \widetilde{\sum_{p^0,k^0}} \int_{\mathbf{p},\mathbf{k}} \text{tr}\,[S_\ell(p)S_{e_R}(k)]\,\Delta_\varphi(p-k+i\omega_n u)$$

$$+(i\omega_n \to -i\omega_n), \tag{3.5}$$

with $u = (1,\mathbf{0})$ the four-velocity of the plasma. We write the scalar field propagator as

$$\Delta_a(p) = \frac{-1}{(v\cdot p)(\overline{v}\cdot p) - \mathbf{p}_\perp^2 - m_a^2}. \tag{3.6}$$

Here, $v = (1,\mathbf{v})$ with a unit vector $\mathbf{v}$, which defines the longitudinal direction, and $\overline{v} = (1,-\mathbf{v})$. Chiral symmetry is unbroken, even with thermal masses. Therefore the non-vanishing components of the fermion propagators in the Weyl representation can be written as 2×2 matrices,

$$S_\ell(p) = \sigma\cdot p\,\Delta_\ell(p), \tag{3.7}$$
$$S_{e_R}(p) = \overline{\sigma}\cdot p\,\Delta_{e_R}(p), \tag{3.8}$$

where σ^μ, $\overline{\sigma}^\mu$ are the usual Pauli matrices. There are two different kinematic situations which we have to take into account: either all momenta satisfy $v\cdot p \sim g^2 T$, $\overline{v}\cdot p \sim T$ or the same but with $v \leftrightarrow \overline{v}$. The second case gives the same result as the first but with $i\omega_n \to -i\omega_n$. For $v\cdot p \sim g^2 T$ the scalar propagator can be approximated as

$$\Delta_a(p) = \frac{1}{2p_\parallel}D_a(p) \tag{3.9}$$

where $p_\parallel \equiv \mathbf{v}\cdot\mathbf{p}$ is the large component of $\mathbf{p}$, and

$$D_a(p) \equiv \frac{-1}{v\cdot p - (\mathbf{p}_\perp^2 + m_a^2)/(2p_\parallel)}. \tag{3.10}$$

Similarly, the fermion propagators can be written as (see e.g. [10])

$$S_\ell(p) = \eta(\mathbf{p})\eta^\dagger(\mathbf{p})\,D_\ell(p), \tag{3.11}$$
$$S_{e_R}(p) = \chi(\mathbf{p})\chi^\dagger(\mathbf{p})\,D_{e_R}(p) \tag{3.12}$$

with the spinors

$$\eta(\mathbf{p}) = \left[1 - \frac{1}{2p_\parallel}(\boldsymbol{\sigma}\cdot\mathbf{p}_\perp)\right]\begin{pmatrix}0\\1\end{pmatrix}, \tag{3.13}$$

$$\chi(\mathbf{p}) = \left[1 + \frac{1}{2p_\parallel}(\boldsymbol{\sigma}\cdot\mathbf{p}_\perp)\right]\begin{pmatrix}1\\0\end{pmatrix}. \tag{3.14}$$

In (3.11) through (3.14) we keep only the leading order contributions to the equilibration rate. It is convenient to associate the spinors in (3.11), (3.12) with the adjacent vertices rather than with the propagators.

After performing the sum over Matsubara frequencies we encounter a factor

$$\mathscr{F}(p_\|, k_\|) = f'_{\mathrm{F}}(k_\|) \left[f_{\mathrm{F}}(p_\|) + f_{\mathrm{B}}(p_\| - k_\|) \right]. \tag{3.15}$$

We can then analytically continue $i\omega_n$ to arbitrary complex ω which gives

$$\Pi_{L_{e\mathrm{R}}L_{e\mathrm{R}}}(\omega) = 2h_e^2 V \int_{\mathbf{k},\mathbf{p}} \frac{\mathscr{F}(p_\|, k_\|)}{k_\| - p_\|} \eta^\dagger(\mathbf{p})\chi(\mathbf{k})\chi^\dagger(\mathbf{k})\eta(\mathbf{p}) \frac{\delta E}{\delta E - \omega} + (\omega \to -\omega), \tag{3.16}$$

where

$$\delta E = \delta E(\mathbf{p}_\perp, \mathbf{k}_\perp) \equiv \frac{m_{e_{\mathrm{R}}}^2 + \mathbf{k}_\perp^2}{2k_\|} - \frac{m_\ell^2 + \mathbf{p}_\perp^2}{2p_\|} - \frac{m_\varphi^2 + (\mathbf{k}_\perp - \mathbf{p}_\perp)^2}{2(k_\| - p_\|)} \tag{3.17}$$

is the change of energy in the decay $\varphi \to \ell\,\bar{e}_{\mathrm{R}}$. When we take the imaginary part of the retarded correlator

$$\Pi_{L_{e\mathrm{R}}L_{e\mathrm{R}}}^{\mathrm{ret}}(\omega) = \Pi_{L_{e\mathrm{R}}L_{e\mathrm{R}}}(\omega + i0^+) \tag{3.18}$$

with ω real, δE becomes equal to $\pm\omega$. For both signs one obtains the same imaginary part. Since we need this to compute the rate using (2.2) we can drop terms of order ω^2 and higher. Pulling out a factor $\eta^\dagger(\mathbf{p})\chi(\mathbf{k})$, corresponding to the leftmost vertex in figure 2 (without gauge bosons) we may write

$$\mathrm{Im}\Pi_{L_{e\mathrm{R}}L_{e\mathrm{R}}}^{\mathrm{ret}}(\omega) = 8h_e^2 V \omega \mathrm{Im} \int_{\mathbf{k},\mathbf{p}} \frac{\mathscr{F}(p_\|, k_\|)}{k_\| - p_\|} \eta^\dagger(\mathbf{p})\chi(\mathbf{k})\, j(\mathbf{p}_\perp, \mathbf{k}_\perp) \tag{3.19}$$

where j satisfies

$$\left(\delta E - i0^+ \right) j(\mathbf{p}_\perp, \mathbf{k}_\perp) = \frac{1}{2}\chi^\dagger(\mathbf{k})\eta(\mathbf{p}). \tag{3.20}$$

Note that in the integrand of (3.19) the delta function $\delta(\delta E)$ appears which enforces energy conservation for the (inverse) Higgs decay. The coefficient Γ is then obtained by plugging (3.19) into (2.7).

3.2 Multiple soft gauge boson scattering

Now we include the effect of multiple scattering mediated by soft gauge bosons, as sketched in figure 2.[4] The result can again be described by (3.19), where j now satisfies

$$\begin{aligned}
\delta E(\mathbf{p}_\perp, \mathbf{k}_\perp)\, j(\mathbf{p}_\perp, \mathbf{k}_\perp) &- i\int \frac{d^2 q_\perp}{(2\pi)^2} \Big\{ \mathscr{C}(\mathbf{q}_\perp^2) \big[j(\mathbf{p}_\perp, \mathbf{k}_\perp) - j(\mathbf{p}_\perp - \mathbf{q}_\perp, \mathbf{k}_\perp) \big] \\
&+ \mathscr{C}'(\mathbf{q}_\perp^2) \Big(y_\varphi y_\ell \big[j(\mathbf{p}_\perp, \mathbf{k}_\perp) - j(\mathbf{p}_\perp - \mathbf{q}_\perp, \mathbf{k}_\perp) \big] \\
&\qquad + y_\ell\, y_{e_{\mathrm{R}}} \big[j(\mathbf{p}_\perp, \mathbf{k}_\perp) - j(\mathbf{p}_\perp - \mathbf{q}_\perp, \mathbf{k}_\perp - \mathbf{q}_\perp) \big] \\
&\qquad - y_\varphi\, y_{e_{\mathrm{R}}} \big[j(\mathbf{p}_\perp, \mathbf{k}_\perp) - j(\mathbf{p}_\perp, \mathbf{k}_\perp - \mathbf{q}_\perp) \big] \Big) \Big\} = \frac{1}{2}\chi^\dagger(\mathbf{k})\eta(\mathbf{p}). \tag{3.21}
\end{aligned}$$

---

[4]The range of the gauge interactions is one power of g smaller than the mean free path of the fermions and the Higgs. Therefore crossed gauge bosons, rainbow self-energies, or gauge boson vertex corrections do not contribute at leading order.
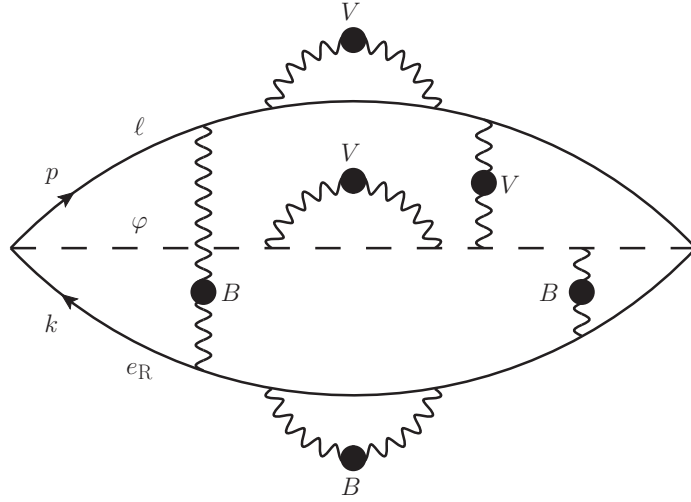
Figure 2. Typical diagram of multiple soft scattering the imaginary part of which gives a contribution to the equilibration rate. V stands for either a W or a hypercharge gauge boson B. All gauge bosons are soft and their propagators are hard thermal loop (HTL) resummed, as indicated by the thick dots.

Here $\mathbf{q}_\perp$ is the transverse momentum of an exchanged gauge boson. We have introduced

$$\mathscr{C}(\mathbf{q}_\perp^2) \equiv \frac{3}{4} g^2 T \left(\frac{1}{\mathbf{q}_\perp^2} - \frac{1}{\mathbf{q}_\perp^2 + m_{\mathrm{D}}^2} \right), \tag{3.22}$$

$$\mathscr{C}'(\mathbf{q}_\perp^2) \equiv g'^2 T \left(\frac{1}{\mathbf{q}_\perp^2} - \frac{1}{\mathbf{q}_\perp^2 + m_{\mathrm{D}}'^2} \right) \tag{3.23}$$

with the Debye masses [26]

$$m_{\mathrm{D}}^2 = \frac{11}{6} g^2 T^2, \qquad m_{\mathrm{D}}'^2 = \frac{11}{6} g'^2 T^2. \tag{3.24}$$

In the integral in (3.21) the terms containing $j(\mathbf{p}_\perp, \mathbf{k}_\perp)$ correspond to self-energy insertions, which can be easily checked by an explicit calculation.[5] The terms with $\mathscr{C}$ and $\mathscr{C}'$ correspond to interactions mediated by W or B bosons, respectively. By themselves, the self-energies are infrared divergent due to the $1/\mathbf{q}_\perp^2$ term in $\mathscr{C}$ and $\mathscr{C}'$. The subtracted terms in the square brackets in (3.21) correspond to gauge boson exchange between different particles and render the $\mathbf{q}_\perp$-integrals finite. The first two square brackets in (3.21) also appear in the computation of the production rate of ultrarelativistic sterile neutrinos [10]. The other two represent the exchange of weak hypercharge gauge bosons by the right-handed electrons. Replacing the integral in (3.21) by 0^+, one neglects multiple soft scatterings and one recovers the equation (3.20) describing Higgs decay.

Thanks to three-dimensional rotational invariance, the solution to (3.21) can be found as a function of a single transverse momentum [27],

$$j(\mathbf{p}_\perp, \mathbf{k}_\perp) = J(\mathbf{P}), \tag{3.25}$$

---

[5] Note that $y_\varphi y_\ell + y_\ell y_{e_{\mathrm{R}}} - y_\varphi y_{e_{\mathrm{R}}} = \left(y_\varphi^2 + y_\ell^2 + y_{e_{\mathrm{R}}}^2 \right)/2.$

with

$$\mathbf{P} \equiv x_k \mathbf{p}_\perp - x_p \mathbf{k}_\perp, \tag{3.26}$$

$$x_k \equiv \frac{k_\parallel}{p_\parallel - k_\parallel}, \qquad x_p \equiv \frac{p_\parallel}{p_\parallel - k_\parallel}. \tag{3.27}$$

In fact, (3.17) now takes the simple form

$$\delta E = \beta \left(\mathbf{P}^2 + M^2 \right) \tag{3.28}$$

with

$$\beta \equiv \frac{p_\parallel - k_\parallel}{2 p_\parallel k_\parallel}, \tag{3.29}$$

and

$$M^2 \equiv \beta^{-1} \left[\frac{m_{e_\mathrm{R}}^2}{2k_\parallel} - \frac{m_\ell^2}{2p_\parallel} - \frac{m_\varphi^2}{2(k_\parallel - p_\parallel)} \right]. \tag{3.30}$$

The right-hand side of (3.21) turns into

$$\frac{1}{2} \chi^\dagger(\mathbf{k}) \eta(\mathbf{p}) = -\frac{\beta}{2} \left(P_x - i P_y \right). \tag{3.31}$$

The function $J(\mathbf{P})$ can be expressed as

$$J(\mathbf{P}) = \frac{i\beta}{4} \left[f_x(\mathbf{P}) - i f_y(\mathbf{P}) \right], \tag{3.32}$$

where the two-component vector $\mathbf{f}$ is a solution to

$$
\begin{aligned}
-i\delta E\, \mathbf{f}(\mathbf{P}) - \int \frac{d^2 q_\perp}{(2\pi)^2} \Big\{ & \mathscr{C}(\mathbf{q}_\perp^2) \big[\mathbf{f}(\mathbf{P}) - \mathbf{f}(\mathbf{P} - x_k \mathbf{q}_\perp) \big] \\
& + \mathscr{C}'(\mathbf{q}_\perp^2) \Big(y_\varphi y_\ell \big[\mathbf{f}(\mathbf{P}) - \mathbf{f}(\mathbf{P} - x_k \mathbf{q}_\perp) \big] \\
& \qquad + y_\ell\, y_{e_\mathrm{R}} \big[\mathbf{f}(\mathbf{P}) - \mathbf{f}(\mathbf{P} + \mathbf{q}_\perp) \big] \\
& \qquad - y_\varphi\, y_{e_\mathrm{R}} \big[\mathbf{f}(\mathbf{P}) - \mathbf{f}(\mathbf{P} + x_p \mathbf{q}_\perp) \big] \Big) \Big\} = 2\mathbf{P}.
\end{aligned}
\tag{3.33}
$$

This is the same integral equation as in [10] (with the appropriate hypercharge assignments), but with two additional terms representing the gauge interaction of right-handed electrons.

Now we choose the unit vector $\mathbf{v}$ in the direction of $\mathbf{k}$. Using $\mathbf{f}(\mathbf{P}) \propto \mathbf{P}$ and integrating over the transverse momentum $\mathbf{k}_\perp$, we obtain

$$\Gamma^{\mathrm{LPM}} = \frac{h_e^2}{8\pi^3} \int\limits_0^\infty dk \int\limits_{-\infty}^\infty dp_\parallel \frac{\left(p_\parallel - k \right)^3}{p_\parallel^2 k^2} \mathscr{F}(p_\parallel, k) \, \mathrm{Re} \int \frac{d^2 P}{(2\pi)^2} \mathbf{P} \cdot \mathbf{f}(\mathbf{P}) \tag{3.34}$$

for the rate coefficient. We solve (3.33) using the algorithm described in [10] and numerically integrate (3.34) (see appendix B).
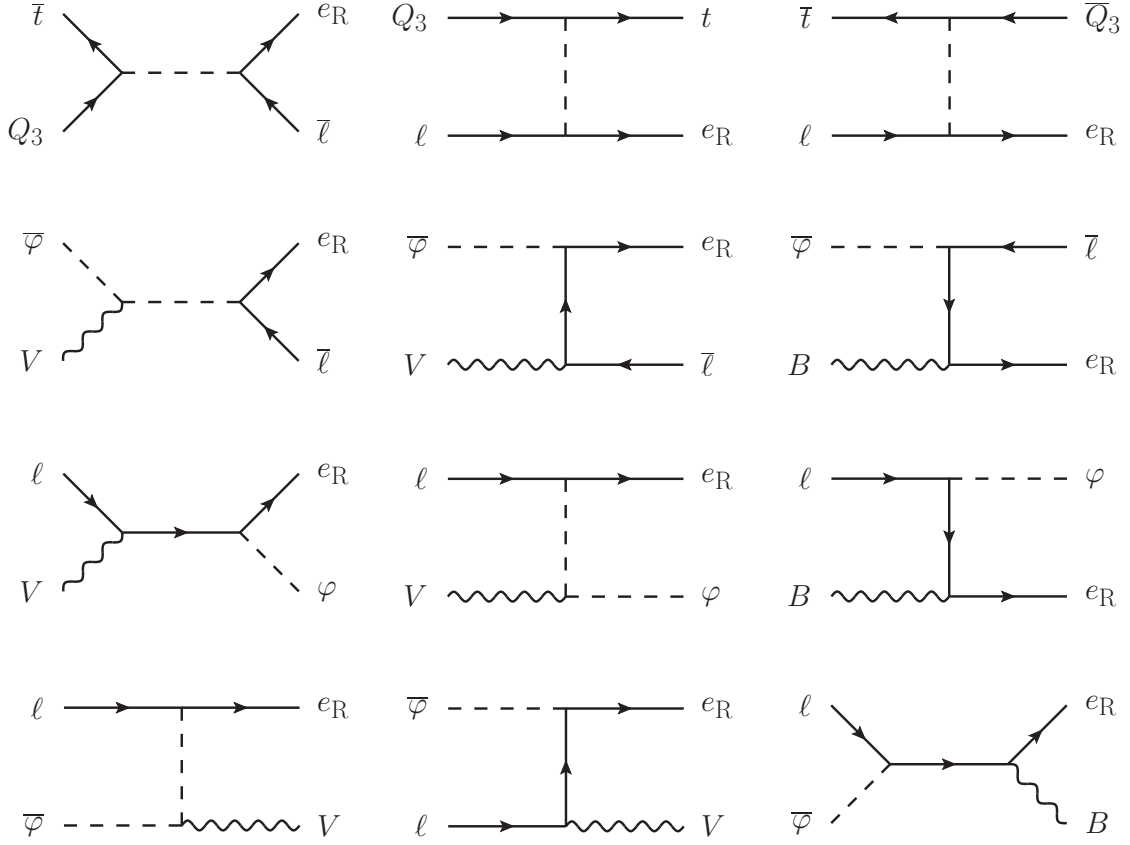
Figure 3. Diagrams for the $2 \to 2$ processes. First line: quark contributions, second line: $V\overline{\varphi} \to \overline{\ell}e_{\mathrm{R}}$, third line: $V\ell \to \varphi e_{\mathrm{R}}$, fourth line: $\ell\overline{\varphi} \to Ve_{\mathrm{R}}$. Here and in the diagrams we denote $V = B, W$. The exchanged fermion in t-channel is an ℓ in the second column and an e_{R} in the third column.

4 $2 \to 2$ processes

At order $h_e^2 g^2$ there are also contributions from $2 \to 2$ scatterings. The corresponding diagrams are shown in figure 3. At leading order all external particles have hard momenta, $p \sim T$, and one can neglect their thermal masses. For s-channel exchange the internal momenta are hard as well, and one can neglect thermal effects on the propagators.[6] However, momenta exchanged in the t-channel become soft at leading order. We treat these contributions in section 4.2.

Again, the processes are similar to the ones encountered in relativistic sterile neutrino production in [9]. However, as in the case of the $1n \leftrightarrow 2n$ processes, in e_{R} equilibration one encounters diagrams in which the produced particle itself couples to a gauge boson B, which leads to additional terms in the matrix elements. In particular, the exchanged particle can be an e_{R} which can become soft in the t-channel. This contribution has to be treated separately.

---

[6]In [2] the thermal Higgs mass is included in the Higgs propagator for the process $\overline{t}Q_3 \to \ell e_{\mathrm{R}}$. This leads to the complication that the propagator can become on-shell, and a subtraction has to be performed. This problem does not arise in a strict leading order calculation.

4.1 Hard momentum transfer

We first consider the case that the exchanged particles have hard momenta. Then the equilibration rate can be determined via the Boltzmann equation [28, 29]. We can write the time derivative of the $L_{e\mathrm{R}}$ density as

$$\dot{n}_{L_{e\mathrm{R}}} = \int_{\mathbf{k}} \frac{\partial}{\partial t} \left[f_{\mathbf{k}} - \bar{f}_{\mathbf{k}} \right] \tag{4.1}$$

where $f_{\mathbf{k}}$ and $\bar{f}_{\mathbf{k}}$ are the occupation numbers of right-handed electrons and positrons. We replace the time derivatives on the right-hand side by the collision term for $2 \to 2$ particle scattering. It contains the occupancies of the participating particles in the form

$$f_1 f_2 [1 \pm f_3][1 - f_{\mathbf{k}}] - [1 \pm f_1][1 \pm f_2] f_3 f_{\mathbf{k}}, \tag{4.2}$$

corresponding to gain and loss term. The upper and lower signs are for bosons and fermions, respectively.

All Standard Model particles are in kinetic equilibrium due to their gauge interactions. Therefore their occupancies are determined by the temperature and by the chemical potentials of the slowly varying charges and of the strictly conserved ones. To compute Γ at lowest order in chemical potentials, we can put all chemical potentials except $\mu_{e_{\mathrm{R}}}$ equal to zero. For the occupancy of right-handed electrons we can therefore write

$$f_{\mathbf{k}} = f_{\mathrm{F}}(k^0 - \mu_{e_{\mathrm{R}}}) \tag{4.3}$$

with $k^0 = |\mathbf{k}|$, $\mu_{e_{\mathrm{R}}} = \mu_{L_{e\mathrm{R}}}$, and for the other Standard Model particles

$$f_i = f_{\mathrm{B,F}}(p_i^0). \tag{4.4}$$

In thermal equilibrium the gain and the loss term cancel,

$$f_1 f_2 [1 \pm f_3][1 - f_{\mathrm{F}}(k^0)] - [1 \pm f_1][1 \pm f_2] f_3 f_{\mathrm{F}}(k^0) = 0, \tag{4.5}$$

so that the collision term vanishes. Expanding to first order in $\mu_{e_{\mathrm{R}}}$ and making use of (4.5) together with

$$f_{\mathrm{F}}' = -\frac{1}{T} f_{\mathrm{F}}[1 - f_{\mathrm{F}}], \tag{4.6}$$

the contribution to the rate coefficient becomes

$$\Gamma^{2\to2,\mathrm{hard}} = \frac{2}{T} \sum_{\mathrm{processes}} \int_{\mathbf{k},\mathbf{p}_1,\mathbf{p}_2,\mathbf{p}_3} \frac{\sum |\mathscr{M}|^2}{16 p_1^0 p_2^0 p_3^0 k^0} (2\pi)^4 \delta^{(4)}(p_1 + p_2 - p_3 - k)$$
$$f_1 f_2 [1 \pm f_3][1 - f_{\mathrm{F}}(k^0)] \Big|_{\mathrm{hard}}. \tag{4.7}$$

Both terms on the right-hand side of (4.1) give the same contribution which gives rise to the factor 2.

One can write (4.7) in terms of the e_{R}-production rate at vanishing e_{R}-density,

$$\Gamma^{2\to2,\mathrm{hard}} = \frac{2}{T} \int_{\mathbf{k}} \left[1 - f_{\mathrm{F}}(k^0)\right] (2\pi)^3 \frac{dn_{e_{\mathrm{R}}}}{dt\,d^3k} \bigg|_{n_{e_{\mathrm{R}}}=0,\,\mathrm{hard}}, \tag{4.8}$$

which is closely related to the production rate of sterile neutrinos computed in [9]. The difference between the two processes is that the sterile neutrinos have no Standard Model gauge interactions, and therefore do not interact once they are produced (at LO in their Yukawa couplings). In contrast, the right-handed electrons carry weak hypercharge. Scatterings mediated by soft hypercharge gauge bosons contribute to the LO rate, as discussed in section 3. However for the $2 \to 2$ scattering of hard particles the soft scattering is a higher order effect and can be neglected here.

The diagrams contributing to the e_R-production are shown in figure 3. The matrix elements for the processes with quarks and W bosons can be read off from [9] by setting $g' \to 0$,

$$\text{quarks} \quad : \quad \Sigma|\mathscr{M}|^2 = 6\,h_t^2\,h_e^2, \tag{4.9}$$

$$W\overline{\varphi} \to \overline{\ell}e_R \quad : \quad \Sigma|\mathscr{M}|^2 = 3g^2\,h_e^2\,\frac{u}{t}, \tag{4.10}$$

$$W\ell \to \varphi e_R \quad : \quad \Sigma|\mathscr{M}|^2 = 3g^2\,h_e^2\,\frac{-u}{s}, \tag{4.11}$$

$$\ell\overline{\varphi} \to We_R \, : \quad \Sigma|\mathscr{M}|^2 = 3g^2\,h_e^2\,\frac{s}{-t}, \tag{4.12}$$

where (4.9) holds for any of the processes $\overline{t}Q_3 \to \ell e_R$, $Q_3\ell \to te_R$, $\overline{t}\ell \to \overline{Q}_3 e_R$. For the processes with hypercharge gauge bosons we find

$$B\overline{\varphi} \to \overline{\ell}e_R \quad : \quad \Sigma|\mathscr{M}|^2 = g'^2\,h_e^2\left[4 + \frac{u}{t} + \frac{4t}{u}\right], \tag{4.13}$$

$$B\ell \to \varphi e_R \quad : \quad \Sigma|\mathscr{M}|^2 = g'^2\,h_e^2\left[-4 + \frac{-u}{s} + \frac{4s}{-u}\right], \tag{4.14}$$

$$\ell\overline{\varphi} \to Be_R \, : \quad \Sigma|\mathscr{M}|^2 = g'^2\,h_e^2\left[-4 + \frac{s}{-t} + \frac{4(-t)}{s}\right]. \tag{4.15}$$

Here we have summed over polarizations, color and weak isospin. The Boltzmann equation can now be integrated as in [9], with some additional integrals due to the terms containing a factor 4 in (4.13) through (4.15). We rewrite the contributions proportional to $1/(-u)$ as a process proportional to $1/(-t)$ by interchanging the incoming particles, which may change the statistics of particles 1 and 2.

In the integrals describing lepton exchange in t-channel we need to handle the infrared divergence appearing when the momentum of the exchanged lepton becomes small. We proceed as in [9] by introducing a transverse momentum cutoff q_{cut} for the exchanged particle with $gT \ll q_{\text{cut}} \ll T$. We isolate the piece which is singular for $q_{\text{cut}} \to 0$ and integrate it analytically. Its logarithmic q_{cut} dependence drops out when combined with the soft contribution (see section 4.2) which includes only transverse momenta less than q_{cut}. The remaining finite integral is then computed numerically.

4.2 Soft momentum transfer

The soft contribution is obtained from the retarded correlator using (2.7), where either of the lepton propagators is HTL resummed. The corresponding diagrams are shown in figure 4. A straightforward computation in imaginary time, in which we make use of the sum rule found in [9], and analytic continuation to real frequency leads to

$$\Gamma^{\text{soft}} = \frac{h_e^2\,T}{64\,\pi}\left[m_\ell^2 \log\left(\frac{q_{\text{cut}}}{m_\ell}\right) + m_{e_R}^2 \log\left(\frac{q_{\text{cut}}}{m_{e_R}}\right)\right]. \tag{4.16}$$
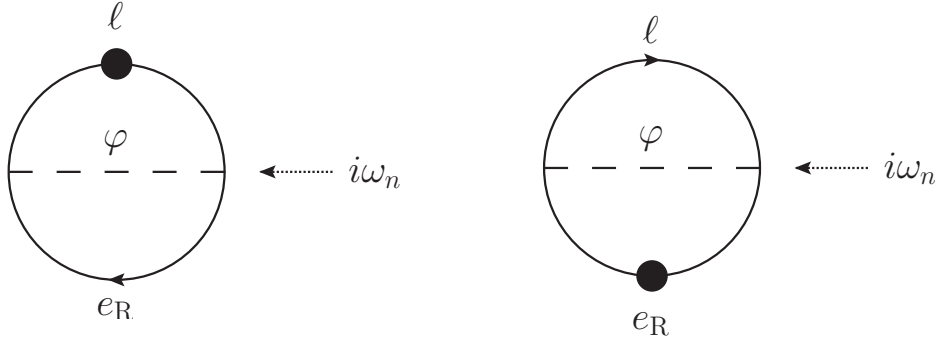
Figure 4. Imaginary time correlator of the time derivative of L_{eR} with one soft fermion. The corresponding propagator has to be HTL resummed. The diagrams with $i\omega_n \to -i\omega_n$ are not shown.

4.3 Complete $2 \to 2$ rate

Adding the hard singular and finite as well as the soft contributions, $q_{\rm cut}$ drops out, and the contribution from $2 \to 2$ scatterings to the rate coefficient Γ is finite. Evaluating the remaining integrals numerically, we find

$$\Gamma^{2\to2} = \frac{h_e^2 T^3}{2048\,\pi} \left\{ h_t^2 c_t + \left(3g^2 + g'^2\right) \left[c_\ell + \log\frac{1}{3g^2 + g'^2} \right] + 4g'^2 \left[c_{e_{\rm R}} + \log\frac{1}{4g'^2} \right] \right\} \quad (4.17)$$

with

$$c_t = 2.82, \qquad c_\ell = 3.52, \qquad c_{e_{\rm R}} = 2.69. \quad (4.18)$$

5 Results and discussion

For our numerical results we evaluate the 1-loop running couplings at the renormalization scale πT. We have checked that increasing the renormalization scale by a factor 2 changes our results by less than 3% in the entire temperature range we consider.

Figure 5 shows the various contributions to the equilibration rate. The $2 \to 2$ processes are dominant over the entire temperature range considered. The largest contribution comes from scatterings off hard gauge bosons. The $1n \leftrightarrow 2n$ contribution is about a factor 0.4 smaller than the total $2 \to 2$ rate. Except at very low temperature the (inverse) Higgs decay gives a negligible contribution, and it vanishes completely above $T \simeq 60\,\text{TeV}$. In table 1 we show numerical values for the total $2 \to 2$ as well as the LPM resummed contribution along with the full result for Γ.

The LPM resummed rate is a complicated function of the coupling constants and there is not such a simple expression like (4.17) for the $2 \to 2$ rate. Inspired by the form of (4.17) we have fitted the LPM contribution with a similar expression,

$$\Gamma^{\rm LPM} \approx \frac{h_e^2 T^3}{2048\,\pi} \left\{ h_t^2 d_t + (3g^2 + g'^2)d_\ell + 4g'^2 d_{e_{\rm R}} \right\}. \quad (5.1)$$

We find that with

$$d_t = 1.48, \qquad d_\ell = 0.776, \qquad d_{e_{\rm R}} = 2.03 \quad (5.2)$$

the relative error of $\Gamma^{\rm LPM}$ is much smaller than our numerical uncertainty throughout the temperature range $10^3\,\text{GeV} \le T \le 10^9\,\text{GeV}$.
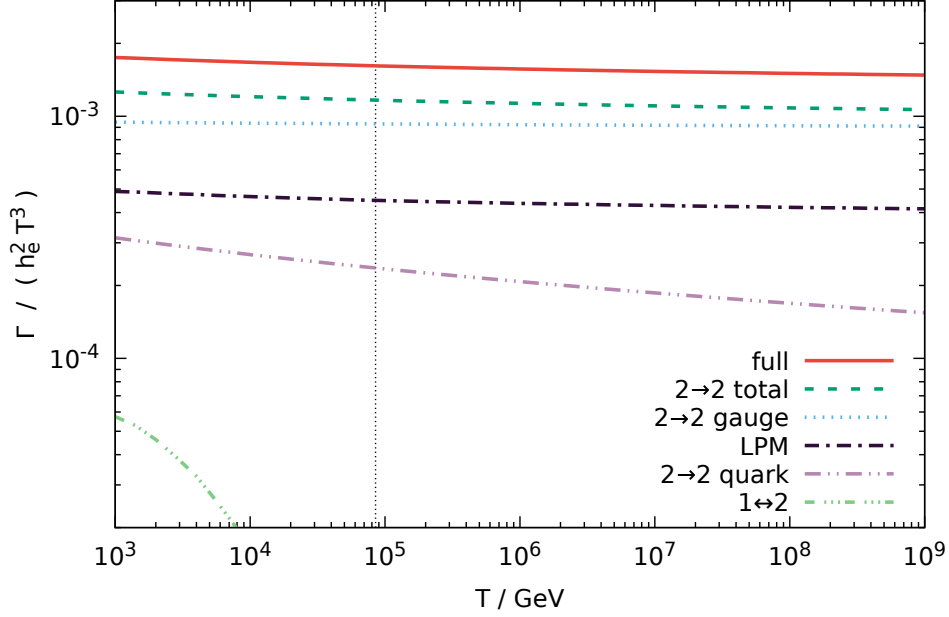
– 15 –

Figure 5. The rate coefficient Γ as function of the temperature. The curve labeled 'full' incorporates all leading order contributions, '$2 \to 2$ total' shows the full result of (4.17) whose contributions by gauge and quark scattering we show as '$2 \to 2$ gauge' and '$2 \to 2$ quark,' respectively. The curve labeled 'LPM' shows the result of (3.34) and is the sum of the resummation of $1n \leftrightarrow 2n$ scatterings by soft gauge boson exchanges and the (inverse) Higgs decay labeled '$1 \leftrightarrow 2$'. The dotted vertical line denotes the equilibration temperature (5.4).

T/GeV	$\Gamma^{2\to2}/(h_e^2 T^3)$	$\Gamma^{\mathrm{LPM}}/(h_e^2 T^3)$	$\Gamma/(h_e^2 T^3)$
$1.00 \cdot 10^3$	$1.26 \cdot 10^{-3}$	$4.89 \cdot 10^{-4}$	$1.75 \cdot 10^{-3}$
$4.00 \cdot 10^3$	$1.22 \cdot 10^{-3}$	$4.75 \cdot 10^{-4}$	$1.70 \cdot 10^{-3}$
$1.60 \cdot 10^4$	$1.19 \cdot 10^{-3}$	$4.62 \cdot 10^{-4}$	$1.65 \cdot 10^{-3}$
$6.40 \cdot 10^4$	$1.17 \cdot 10^{-3}$	$4.51 \cdot 10^{-4}$	$1.62 \cdot 10^{-3}$
$2.56 \cdot 10^5$	$1.15 \cdot 10^{-3}$	$4.43 \cdot 10^{-4}$	$1.59 \cdot 10^{-3}$
$1.02 \cdot 10^6$	$1.13 \cdot 10^{-3}$	$4.36 \cdot 10^{-4}$	$1.57 \cdot 10^{-3}$
$4.10 \cdot 10^6$	$1.11 \cdot 10^{-3}$	$4.31 \cdot 10^{-4}$	$1.54 \cdot 10^{-3}$
$1.64 \cdot 10^7$	$1.10 \cdot 10^{-3}$	$4.26 \cdot 10^{-4}$	$1.53 \cdot 10^{-3}$
$6.55 \cdot 10^7$	$1.09 \cdot 10^{-3}$	$4.22 \cdot 10^{-4}$	$1.51 \cdot 10^{-3}$
$2.62 \cdot 10^8$	$1.07 \cdot 10^{-3}$	$4.18 \cdot 10^{-4}$	$1.49 \cdot 10^{-3}$
$1.05 \cdot 10^9$	$1.06 \cdot 10^{-3}$	$4.14 \cdot 10^{-4}$	$1.47 \cdot 10^{-3}$

Table 1. Numerical values of the contributions from $2 \to 2$ and LPM resummed multiple soft scattering to the equilibration rate coefficient Γ. The numerical uncertainty in the LPM contribution is below 2%.

T	10^3 GeV	10^6 GeV	10^9 GeV
LPM	21%	30%	39%
$2 \to 2$	34%	44%	53%
total	30%	40%	49%

Table 2. Relative increase of Γ when hypercharge gauge interactions are included.

The right-handed electron lepton number comes into equilibrium around the temperature T_{eq} at which γ equals the Hubble rate[7]

$$H = \sqrt{\frac{4\pi^3 g_*}{45}} \frac{T^2}{m_{\mathrm{Pl}}}. \tag{5.3}$$

Here g_* is the number of relativistic degrees of freedom with $g_* = 106.75$ in the Standard Model, $m_{\mathrm{Pl}} = 1.22 \cdot 10^{19}$ GeV is the Planck mass. Using (2.22) we find for the equilibration temperature T_{eq} of the right-handed electron lepton number in the Standard Model

$$T_{\mathrm{eq}} = 8.5 \cdot 10^4 \, \mathrm{GeV}. \tag{5.4}$$

This value lies in the temperature region in which leptogenesis through neutrino oscillations [3, 4] can take place, see e.g. [30, 31]. In this case X_α and $L_{e\mathrm{R}}$ are violated on similar time scales, and the kinetic equations must describe the evolution of all four quantities.

It is interesting to see how hypercharge gauge interactions affect the e_{R}-equilibration, since they give rise to diagrams which are not present in sterile neutrino production. We find that they substantially boost the equilibration rate. In table 2 we show the increase in the complete rate compared to the result with $g' = 0$. Despite the relative smallness of g', its effect on the equilibration rate is quite significant, and it increases with the temperature due to the different running of g' and g.

The first calculation of the e_{R}-equilibration rate was performed in [1], where only the $2 \to 1$ inverse Higgs decay is taken into account and thermal fermion masses as well as the final state distribution function are neglected. At $T = 10^3$ GeV our result is about 5 times as large as the one obtained in [1]. Around the equilibration temperature (5.4) the inverse decay is not even kinematically allowed when thermal fermion masses are included, here we obtain a result that is about 6 times the one obtained by the approximations of [1].

Reference [2] includes $2 \leftrightarrow 2$ processes as well as the (inverse) Higgs decays while neglecting $1n \leftrightarrow 2n$ scattering. We can compare the $2 \to 2$ scattering rates involving quarks. Therefore we recompute c_t in (4.17) using Maxwell-Boltzmann statistics for all particles, leading to $c_t^{\mathrm{MB}} = 2.14$, which is a relative error of 24% compared to the correct quantum statistics, as anticipated in [2]. Our result for classical statistics is 9% larger than the one obtained in [2]. We can also compare the gauge contribution to the $2 \to 2$ scatterings. With the values for the gauge couplings of [2], our result is about 50% larger[8] which could be due to the use of classical statistics and of zero-momentum thermal fermion masses in [2].

The equilibration of right-handed muons and taus in a temperature regime between 10^7 and 10^{13} GeV is considered in [7], by including the (inverse) Higgs decays and $2 \leftrightarrow 2$ scatterings. By removing the inverse susceptibilities and the slow Yukawa couplings, we

---

[7]In [2] a different definition of the e_{R} equilibration temperature is used.
[8]Cf. equations (25) through (27) in [2].

can compare our results for Γ/h_e^2, because it is lepton-flavor independent. We find our full rate to be 2.8 times their result. The authors also estimate the effect of multiple soft scattering.[9] The relative magnitude of the effect of multiple soft scattering is estimated in [7] as $\gamma^{\mathrm{LPM}}/\gamma^{2\to2} \sim 0.25$, while we obtain about 0.4. Our result for the quark contribution to $2 \to 2$ scattering is 2 times the result in [7], and both our logarithmic contributions to $\Gamma^{2\to2}$ are 2.2 times as large as the ones in [7].

To summarize, we have computed the equilibration rate of right-handed electrons in the symmetric phase by including, for the first time, all Standard Model processes at leading order in the couplings. We have found that the dominant processes are $2 \to 2$ scatterings. Leading order contributions are also given by inverse Higgs decays and additional soft scattering which was included by Landau-Pomeranchuk-Migdal (LPM) resummation. We obtain an equilibration rate which is substantially larger than approximations presented in previous literature. Our result shows that it can be important to include the process of e_{R} equilibration in low-scale leptogenesis.

Acknowledgments

A Susceptibilities

In this appendix we compute the susceptibilities which relate the chemical potentials to the densities of slowly violated and of strictly conserved charges in (2.9) at leading (zeroth) order in the couplings. When the right-handed electrons come into equilibrium, the μ and τ Yukawa interactions are already fast, so that the lepton numbers carried by the corresponding right-handed particles are not conserved. Having expanded already in h_e, the violation of $L_{e\mathrm{R}}$ is of higher order and we can consider it conserved, hence we introduce a chemical potential $\mu_{L_{e\mathrm{R}}}$. The weak hypercharge Y is strictly conserved. The zero-momentum mode of the temporal component of the hypercharge gauge field B_0 plays the role of the corresponding chemical potential, see (2.16). Integrating over B_0 enforces $Y = 0$. Then the particle chemical potentials read

$$\mu_Q = \frac{1}{6}\mu_Y - \frac{1}{3}\mu_X, \qquad \mu_{u_{\mathrm{R}}} = \frac{2}{3}\mu_Y - \frac{1}{3}\mu_X, \qquad \mu_{d_{\mathrm{R}}} = -\frac{1}{3}\mu_Y - \frac{1}{3}\mu_X$$

$$\mu_{\ell_\alpha} = -\frac{1}{2}\mu_Y + \mu_{X_\alpha}, \qquad \mu_{e_{\mathrm{R}}} = -\mu_Y + \mu_{X_e} + \mu_{L_{e\mathrm{R}}}, \qquad \mu_{\mu_{\mathrm{R}}} = -\mu_Y + \mu_{X_\mu}$$

$$\mu_{\tau_{\mathrm{R}}} = -\mu_Y + \mu_{X_\tau}, \qquad \mu_\varphi = \frac{1}{2}\mu_Y, \tag{A.1}$$

---

[9]See equation (97) in [7].

with $\mu_X \equiv \frac{1}{3} \sum_\alpha \mu_{X_\alpha}$. Now we compute the pressure and obtain the matrix of susceptibilities via (2.10). Inversion of this matrix yields

$$\chi^{-1} = \frac{1}{481\,T^2} \begin{pmatrix} 4266 & -1110 & 312 & 312 & 270 \\ -1110 & 1332 & 0 & 0 & 222 \\ 312 & 0 & 1066 & 104 & 312 \\ 312 & 0 & 104 & 1066 & 312 \\ 270 & 222 & 312 & 312 & 492 \end{pmatrix} \tag{A.2}$$

for the ordering $\{L_{e\mathrm{R}}, X_e, X_\mu, X_\tau, Y\}$.

B Solving the integral equation

The Fourier transformation

$$\mathbf{f}(\mathbf{B}) \equiv \int \frac{d^2 P}{(2\pi)^2} e^{i\mathbf{P}\cdot\mathbf{B}}\,\mathbf{f}(\mathbf{P}) \tag{B.1}$$

turns the integral equation (3.33) for $\mathbf{f}(\mathbf{P})$ into a differential equation for $\mathbf{f}(\mathbf{B})$,

$$i\beta\left(\Delta - M^2\right)\mathbf{f}(\mathbf{B}) = \mathscr{K}(B)\,\mathbf{f}(\mathbf{B}) - 2\,i\,\nabla\delta^{(2)}(\mathbf{B}), \tag{B.2}$$

where the differential operators act on the two-dimensional impact parameter $\mathbf{B}$. We denote $B \equiv |\mathbf{B}|$ and we have introduced

$$\begin{aligned} \mathscr{K}(B) &\equiv \frac{3g^2 T}{4}\mathscr{D}(x_k m_\mathrm{D} B) \\ &\quad + g'^2 T\big[y_\varphi y_\ell\,\mathscr{D}(x_k m_\mathrm{D}' B) + y_\ell y_{e_\mathrm{R}}\,\mathscr{D}\left(m_\mathrm{D}' B\right) - y_\varphi y_{e_\mathrm{R}}\,\mathscr{D}\left(x_p m_\mathrm{D}' B\right)\big] \end{aligned} \tag{B.3}$$

with

$$\mathscr{D}(y) \equiv \frac{1}{2\pi}\left[\gamma_\mathrm{E} + K_0(|y|) + \log\left|\frac{y}{2}\right|\right]. \tag{B.4}$$

γ_E is the Euler-Mascheroni constant and K_0 is a modified Bessel function. In terms of the Fourier transform the real part in (3.34) becomes

$$\mathrm{Re} \int \frac{d^2 P}{(2\pi)^2}\mathbf{P} \cdot \mathbf{f}(\mathbf{P}) = \lim_{\mathbf{B}\to\mathbf{0}} \mathrm{Im}\nabla \cdot \mathbf{f}(\mathbf{B}). \tag{B.5}$$

Writing $\mathbf{f}(\mathbf{B}) \equiv \mathbf{B}\,h(B)$, we arrive at the following ordinary differential equation for $h(B)$, valid at $B \neq 0$,

$$i\beta\left\{\frac{d^2}{dB^2} + \frac{3}{B}\frac{d}{dB} - M^2\right\}h(B) - \mathscr{K}(B)\,h(B) = 0. \tag{B.6}$$

In terms of h, the relation (B.5) becomes

$$\mathrm{Re} \int \frac{d^2 P}{(2\pi)^2}\mathbf{P} \cdot \mathbf{f}(\mathbf{P}) = 2\lim_{B\to0} \mathrm{Im}\,h(B). \tag{B.7}$$

For $B \to 0$ the function h has a singularity which is determined by the delta function in (B.2),

$$h(B) \overset{B \to 0}{\sim} -\frac{1}{\pi \beta B^2}, \tag{B.8}$$

and which is insensitive to $\mathscr{K}$. Being purely real, this singularity does not enter (B.7). We write $h = h^{\mathrm{decay}} + h^{\mathrm{scat}}$, where h^{decay} contains only the (inverse) Higgs decay contribution. We obtain it by solving (3.33) with $\int d^2 q_\perp \{\cdots\} \to 0^+ \, \mathbf{f}(\mathbf{P})$ and then taking the Fourier transform. This gives

$$h^{\mathrm{decay}}(B) = \begin{cases} -\dfrac{m}{\pi \beta B} K_1(mB) & (M^2 > 0) \\[2mm] \dfrac{m}{2\beta B} \left[Y_1(mB) - i \, \mathrm{sign}(\beta) \, J_1(mB) \right] & (M^2 < 0) \end{cases} \tag{B.9}$$

with $m \equiv \sqrt{|M^2|}$, and the (modified) Bessel functions K_1, Y_1 and J_1. Then we solve the differential equation for h^{scat} numerically as described in [10].

C Integrals appearing in the $2 \to 2$ rate

After summing over all leading order processes the production rate on the right-hand side of (4.8) can be written as

$$\left. \frac{dn_{e_{\mathrm{R}}}}{dt \, dk^0} \right|_{n_{e_{\mathrm{R}}}=0} = \frac{h_e^2 f_{\mathrm{F}}(k^0)}{128 \pi^5} \Big[18 \, h_t^2 \, \mathscr{I}_{\mathrm{fff}}^0$$

$$+ (3g^2 + g'^2) \left\{ \mathscr{I}_{\mathrm{bfb}}^1 + \mathscr{I}_{\mathrm{bbf}}^1 + \mathscr{I}_{\mathrm{fbb}}^1 \right\}$$

$$+ 4 g'^2 \left\{ \mathscr{I}_{\mathrm{bfb}}^1 + \mathscr{I}_{\mathrm{bbf}}^1 + \mathscr{I}_{\mathrm{fbb}}^1 + \mathscr{I}_{\mathrm{bbf}}^0 - 2 \mathscr{I}_{\mathrm{bfb}}^0 \right\} \Big] \tag{C.1}$$

with $k^0 = |\mathbf{k}|$. Here we have already integrated over the direction of $\mathbf{k}$. The $\mathscr{I}_{123}^n$ are the different phase space integrals appearing in (4.7). The lower indices refer to the statistics of the particles $1, 2, 3$ and the upper index $n = 0, 1$ is the power of the ratios of Mandelstam variables in equations (4.9)–(4.15). The exact definitions of the $\mathscr{I}$ are given below.

Like in [9] we carry out some integrations analytically until there are two integrals over the variables $q_\pm \equiv (q^0 \pm |\mathbf{q}|)/2$ left. If not stated otherwise, q is the exchanged 4-momentum. For each process we decompose the products of occupancies in (4.7) as

$$f_1 f_2 [1 \pm f_3] = f_{\mathrm{F}}(k^0) \widetilde{f} \widehat{f}, \tag{C.2}$$

where $\widehat{f}$ is a function of $q_+ + q_-$ and of the energy of one incoming particle only. Most of the integrals appear in sterile neutrino production as well. For the sake of completeness, we list them in this appendix, adopted to our notation. We also give the analytic integrals which were not computed in [9]. The terms containing $1/t$ are infrared divergent when integrated over $q_\pm$. All divergent contributions encountered here already appear in sterile neutrino production (see [9] for details).

C.1 $\mathscr{I}_{\mathbf{fff}}$

This integral is exclusive to quark scattering. Since the squared matrix elements do not depend on the Mandelstam variables, we may choose $q = p_3 + k$ for both s- and t-channel. We find

$$\widetilde{f} = f_{\mathrm{B}}(q_+ + q_-) + f_{\mathrm{F}}(q_+ + q_- - k^0) \tag{C.3}$$

$$\widehat{f} = 1 - f_{\mathrm{F}}(q_+ + q_- - E_2) - f_{\mathrm{F}}(E_2), \tag{C.4}$$

and we have

$$\mathscr{I}_{\mathrm{fff}}^0 = \int\limits_{k^0}^{\infty} dq_+ \int\limits_0^{k^0} dq_- \, \widetilde{f} \int\limits_{q_-}^{q_+} dE_2 \, \widehat{f}. \tag{C.5}$$

Only $n = 0$ appears, and the integral of $\widehat{f}$ over E_2 is given by equation (A.10) of [9].

C.2 $\mathscr{I}_{\mathbf{bfb}}$

This integral appears in s-channel processes, so that $q = p_3 + k$. We have

$$\widetilde{f} = f_{\mathrm{F}}(q_+ + q_-) + f_{\mathrm{B}}(q_+ + q_- - k^0) \tag{C.6}$$

$$\widehat{f} = 1 + f_{\mathrm{B}}(q_+ + q_- - E_2) - f_{\mathrm{F}}(E_2), \tag{C.7}$$

and we need

$$\mathscr{I}_{\mathrm{bfb}}^n = \int\limits_{k^0}^{\infty} dq_+ \int\limits_0^{k^0} dq_- \, \widetilde{f} \int\limits_{q_-}^{q_+} dE_2 \, \widehat{f} \left(\frac{\langle -u \rangle}{s} \right)^n \tag{C.8}$$

where $\langle -u \rangle$ is the Mandelstam variable u averaged over angles,

$$\frac{\langle -u \rangle}{s} = \frac{q_+^2 + q_-^2 - (q_+ + q_-)(E_2 + k^0) + 2E_2 k^0}{(q_+ - q_-)^2}. \tag{C.9}$$

The result of the E_2 integration is found in equation (A.13) of [9]. For the $n = 0$ integral we obtain

$$\int\limits_{q_-}^{q_+} dE_2 \, \widehat{f} = -(q_+ - q_-) + T \left[\log\left(-1 + e^{2q_+/T} \right) - \log\left(-1 + e^{2q_-/T} \right) \right]. \tag{C.10}$$

C.3 $\mathscr{I}_{\mathbf{bbf}}$

This function arises in t-channel processes, so that $q = p_1 - p_3$. We obtain

$$\widetilde{f} = 1 + f_{\mathrm{B}}(k^0 - q_+ - q_-) - f_{\mathrm{F}}(q_+ + q_-) \tag{C.11}$$

$$\widehat{f} = f_{\mathrm{B}}(E_1) + f_{\mathrm{F}}(E_1 - q_+ - q_-) \tag{C.12}$$

such that

$$\mathscr{I}_{\mathrm{bbf}}^n = \int\limits_0^{k^0} dq_+ \int\limits_{-\infty}^0 dq_- \, \widetilde{f} \int\limits_{q_+}^{\infty} dE_1 \, \widehat{f} \left(\frac{\langle u \rangle}{t} \right)^n. \tag{C.13}$$

Here we have

$$\frac{\langle u \rangle}{t} = \frac{2q_+ q_- + 2E_1 k^0 - (q_+ + q_-)(E_1 + k^0)}{(q_+ - q_-)^2}. \tag{C.14}$$

The E_1 integral with $n = 1$ is equation (A.24) of [9], while for the case $n = 0$ we get

$$\int\limits_{q_+}^{\infty} dE_1 \, \widehat{f} = q_+ + q_- + T \left[\log\left(1 + e^{-q_-/T}\right) - \log\left(-1 + e^{q_+/T}\right) \right]. \tag{C.15}$$

C.4 $\mathscr{I}_{\mathbf{fbb}}$

We encounter this integral in t-channel, so again $q = p_1 - p_3$. Here

$$\widetilde{f} = 1 + f_B(k^0 - q_+ - q_-) - f_F(q_+ + q_-) \tag{C.16}$$

$$\widehat{f} = f_F(E_1) + f_B(E_1 - q_+ - q_-) \tag{C.17}$$

and we have

$$\mathscr{I}_{\mathrm{fbb}}^1 = \int\limits_0^{k^0} dq_+ \int\limits_{-\infty}^0 dq_- \, \widetilde{f} \int\limits_{q_+}^{\infty} dE_1 \, \widehat{f} \left(\frac{\langle s \rangle}{-t} \right). \tag{C.18}$$

We write $\langle s \rangle/(-t) = 1 + \langle u \rangle/t$ with $\langle u \rangle/t$ from (C.14). We only need $n = 1$, and the corresponding integral over E_1 is found in [9] in (A.20).

D Conversion of $L_{e\mathrm{R}}$ to hypercharge gauge fields

Even without Yukawa interaction the conservation of $L_{e\mathrm{R}}$ is violated by the chiral anomaly[10]

$$\partial_\mu j_{e\mathrm{R}}^\mu = -\frac{y_{e\mathrm{R}}^2 g'^2}{32\pi^2} \varepsilon^{\mu\nu\rho\sigma} F_{\mu\nu} F_{\rho\sigma}, \tag{D.1}$$

with

$$j_{e\mathrm{R}}^\mu \equiv \overline{e_{\mathrm{R}}} \, \gamma^\mu e_{\mathrm{R}}. \tag{D.2}$$

$F_{\mu\nu}$ denotes the hypercharge field strength, and we use the convention $\epsilon^{0123} = +1$. This may lead to interesting effects, such as the generation of primordial magnetic fields [5, 33]. In this appendix we want to see when the anomaly can affect the long time and large distance behavior of $j_{e\mathrm{R}}$. Even if there are no gauge fields present initially, there is an instability in the gauge fields for non-zero $\mu_{L_{e\mathrm{R}}}$, leading to exponential growth [5]. We compute the maximal growth rate of the unstable modes in order to derive a bound on $|\mu_{L_{e\mathrm{R}}}|$, below which the growth is smaller than the equilibration rate γ and can be neglected in the kinetic equation (1.1).

---

[10]One can find different prefactors on the right-hand side of (D.1) in the literature, which are related to different conventions for the weak hypercharge. Ours is the same as in [32].

The hypercharge electric and magnetic fields $\mathbf{E}$ and $\mathbf{B}$ with wavelengths greater than the particle mean free path are described by magneto-hydrodynamics. In the presence of the anomaly (D.1), in addition to the usual ohmic current $\mathbf{j}_{\text{Ohm}} = \sigma \mathbf{E}$ with the hyperelectric conductivity σ, one has to take into account the contribution [5, 34]

$$\mathbf{j}_{\text{anomaly}} = -\frac{y_{e\text{R}}^2 g'^2}{4\pi^2} \mu_{L_{e\text{R}}} \mathbf{B}. \tag{D.3}$$

The fields evolve on time scales much larger than σ^{-1}. Therefore $\dot{\mathbf{E}}$ is much smaller than $\sigma \mathbf{E}$, and can be neglected in the equations of motion which become

$$\mathbf{E} = \frac{1}{\sigma} \left[\nabla \times \mathbf{B} + \frac{y_{e\text{R}}^2 g'^2}{4\pi^2} \mu_{L_{e\text{R}}} \mathbf{B} \right], \tag{D.4}$$

$$\dot{\mathbf{B}} = -\nabla \times \mathbf{E}. \tag{D.5}$$

Using $\nabla \cdot \mathbf{B} = 0$, these can be recast as

$$\dot{\mathbf{B}} + \frac{1}{\sigma} \left[-\triangle \mathbf{B} + \frac{y_{e\text{R}}^2 g'^2}{4\pi^2} \mu_{L_{e\text{R}}} \nabla \times \mathbf{B} \right] = \mathbf{0}. \tag{D.6}$$

Following [5], we Fourier transform $\mathbf{B}(t, \mathbf{x}) = \int_{\mathbf{k}} \mathbf{B}_{\mathbf{k}}(t) e^{i\mathbf{k}\cdot\mathbf{x}}$ to obtain

$$\sigma \dot{\mathbf{B}}_{\mathbf{k}} + \mathbf{k}^2 \mathbf{B}_{\mathbf{k}} + i \frac{y_{e\text{R}}^2 g'^2}{4\pi^2} \mu_{L_{e\text{R}}} \mathbf{k} \times \mathbf{B}_{\mathbf{k}} = \mathbf{0}. \tag{D.7}$$

Now decompose $\mathbf{B}_{\mathbf{k}} = \sum_{i=1}^{2} b_i \mathbf{e}_i$. The $\mathbf{e}_i$ are an orthonormal basis in the plane orthogonal to $\mathbf{k}$. The equations for $b_{\pm} \equiv b_1 \pm i b_2$ decouple,

$$\sigma \dot{b}_{\pm} = -|\mathbf{k}| \left(|\mathbf{k}| \mp \frac{y_{e\text{R}}^2 g'^2}{4\pi^2} \mu_{L_{e\text{R}}} \right) b_{\pm}. \tag{D.8}$$

For

$$|\mathbf{k}| < \frac{y_{e\text{R}}^2 g'^2}{4\pi^2} |\mu_{L_{e\text{R}}}| \tag{D.9}$$

there is an instability with the growth rate

$$\gamma_{\text{inst}} = \frac{|\mathbf{k}|}{\sigma} \left(\frac{y_{e\text{R}}^2 g'^2}{4\pi^2} |\mu_{L_{e\text{R}}}| - |\mathbf{k}| \right). \tag{D.10}$$

The maximal growth rate is

$$\gamma_{\text{inst}}^{\text{max}} = \frac{\mu_{L_{e\text{R}}}^2 y_{e\text{R}}^4 g'^4}{64\pi^4 \sigma}. \tag{D.11}$$

The linear kinetic equation neglecting the dynamics of the long wavelength hypermagnetic fields is valid as long as the magnetic dynamics happen on longer time scales than the perturbative ones characterized by the equilibration rate γ,

$$\gamma_{\text{inst}}^{\text{max}} < \gamma. \tag{D.12}$$

In the leading logarithmic approximation the hyperelectric conductivity is [35]

$$\sigma = C\frac{T}{g'^2 \log(1/g')}, \tag{D.13}$$

with $C = 7.05$ in the Standard Model with one Higgs doublet.[11] At the equilibration temperature (5.4) in the Standard Model, (D.12) translates into the condition (1.2).

Consider again example 3 of section 2.2. Here the constraint (1.2) implies

$$\left| Y_{L_{e\mathrm{R}}} - \frac{1110}{4266} Y_{X_e} + \frac{312}{4266} \left(Y_{X_\mu} + Y_{X_\tau} \right) \right| \lesssim 3.4 \cdot 10^{-6}, \tag{D.14}$$

for the yield parameters $Y_i \equiv n_i/s$ with the entropy density s. The Y_{X_α} are typically on the order of $10^{-9} \ldots 10^{-8}$ [30, 31]. Since the dominant source terms in the kinetic equation for $L_{e\mathrm{R}}$ are the X_α, we expect $Y_{L_{e\mathrm{R}}}$ to be of similar size, and (D.14) is easily satisfied.

References

[1] B.A. Campbell, S. Davidson, J.R. Ellis and K.A. Olive, *On the baryon, lepton flavor and right-handed electron asymmetries of the universe*, *Phys. Lett.* **B 297** (1992) 118 [hep-ph/9302221] [INSPIRE].

[2] J.M. Cline, K. Kainulainen and K.A. Olive, *Protecting the primordial baryon asymmetry from erasure by sphalerons*, *Phys. Rev.* **D 49** (1994) 6394 [hep-ph/9401208] [INSPIRE].

[3] E.K. Akhmedov, V.A. Rubakov and A.Y. Smirnov, *Baryogenesis via neutrino oscillations*, *Phys. Rev. Lett.* **81** (1998) 1359 [hep-ph/9803255] [INSPIRE].

[4] T. Asaka and M. Shaposhnikov, *The νMSM, dark matter and baryon asymmetry of the universe*, *Phys. Lett.* **B 620** (2005) 17 [hep-ph/0505013] [INSPIRE].

[5] M. Joyce and M.E. Shaposhnikov, *Primordial magnetic fields, right-handed electrons and the Abelian anomaly*, *Phys. Rev. Lett.* **79** (1997) 1193 [astro-ph/9703005] [INSPIRE].

[6] M. Beneke, B. Garbrecht, C. Fidler, M. Herranen and P. Schwaller, *Flavoured Leptogenesis in the CTP Formalism*, *Nucl. Phys.* **B 843** (2011) 177 [arXiv:1007.4783] [INSPIRE].

[7] B. Garbrecht, F. Glowna and P. Schwaller, *Scattering Rates For Leptogenesis: Damping of Lepton Flavour Coherence and Production of Singlet Neutrinos*, *Nucl. Phys.* **B 877** (2013) 1 [arXiv:1303.5498] [INSPIRE].

[8] D.G. Figueroa and M. Shaposhnikov, *Anomalous non-conservation of fermion/chiral number in Abelian gauge theories at finite temperature*, *JHEP* **04** (2018) 026 [arXiv:1707.09967] [INSPIRE].

[9] D. Besak and D. Bödeker, *Thermal production of ultrarelativistic right-handed neutrinos: Complete leading-order results*, *JCAP* **03** (2012) 029 [arXiv:1202.1288] [INSPIRE].

[10] A. Anisimov, D. Besak and D. Bödeker, *Thermal production of relativistic Majorana neutrinos: Strong enhancement by multiple soft scattering*, *JCAP* **03** (2011) 042 [arXiv:1012.3784] [INSPIRE].

[11] L.D. Landau and I. Pomeranchuk, *Limits of applicability of the theory of bremsstrahlung electrons and pair production at high-energies*, *Dokl. Akad. Nauk Ser. Fiz.* **92** (1953) 535 [INSPIRE].

[12] L.D. Landau and I. Pomeranchuk, *Electron cascade process at very high-energies*, *Dokl. Akad. Nauk Ser. Fiz.* **92** (1953) 735 [INSPIRE].

[13] A.B. Migdal, *Bremsstrahlung and pair production in condensed media at high-energies*, *Phys. Rev.* **103** (1956) 1811 [INSPIRE].

---

[11]Adding further Higgs doublets decreases the conductivity.

[14] R. Baier, Y.L. Dokshitzer, A.H. Mueller, S. Peigne and D. Schiff, *Radiative energy loss of high-energy quarks and gluons in a finite volume quark-gluon plasma*, *Nucl. Phys.* **B 483** (1997) 291 [hep-ph/9607355] [INSPIRE].

[15] B.G. Zakharov, *Fully quantum treatment of the Landau-Pomeranchuk-Migdal effect in QED and QCD*, *JETP Lett.* **63** (1996) 952 [hep-ph/9607440] [INSPIRE].

[16] P.B. Arnold, G.D. Moore and L.G. Yaffe, *Photon and gluon emission in relativistic plasmas*, *JHEP* **06** (2002) 030 [hep-ph/0204343] [INSPIRE].

[17] D. Bödeker and M. Laine, *Kubo relations and radiative corrections for lepton number washout*, *JCAP* **05** (2014) 041 [arXiv:1403.2755] [INSPIRE].

[18] D. Bödeker and M. Sangel, *Lepton asymmetry rate from quantum field theory: NLO in the hierarchical limit*, *JCAP* **06** (2017) 052 [arXiv:1702.02155] [INSPIRE].

[19] S.Y. Khlebnikov and M.E. Shaposhnikov, *Melting of the Higgs vacuum: Conserved numbers at high temperature*, *Phys. Lett.* **B 387** (1996) 817 [hep-ph/9607386] [INSPIRE].

[20] J. Ghiglieri and M. Laine, *GeV-scale hot sterile neutrino oscillations: a derivation of evolution equations*, *JHEP* **05** (2017) 132 [arXiv:1703.06087] [INSPIRE].

[21] H.A. Weldon, *Effective Fermion Masses of Order gT in High Temperature Gauge Theories with Exact Chiral Invariance*, *Phys. Rev.* **D 26** (1982) 2789 [INSPIRE].

[22] P.B. Arnold, G.D. Moore and L.G. Yaffe, *Photon emission from ultrarelativistic plasmas*, *JHEP* **11** (2001) 057 [hep-ph/0109064] [INSPIRE].

[23] P. Aurenche, F. Gelis, G.D. Moore and H. Zaraket, *Landau-Pomeranchuk-Migdal resummation for dilepton production*, *JHEP* **12** (2002) 006 [hep-ph/0211036] [INSPIRE].

[24] R. Baier, Y.L. Dokshitzer, A.H. Mueller, S. Peigne and D. Schiff, *Radiative energy loss and p_T broadening of high-energy partons in nuclei*, *Nucl. Phys.* **B 484** (1997) 265 [hep-ph/9608322] [INSPIRE].

[25] B.G. Zakharov, *Radiative energy loss of high-energy quarks in finite size nuclear matter and quark-gluon plasma*, *JETP Lett.* **65** (1997) 615 [hep-ph/9704255] [INSPIRE].

[26] M.E. Carrington, *The Effective potential at finite temperature in the Standard Model*, *Phys. Rev.* **D 45** (1992) 2933 [INSPIRE].

[27] P. Arnold and S. Iqbal, *The LPM effect in sequential bremsstrahlung*, *JHEP* **04** (2015) 070 [*Erratum ibid.* **09** (2016) 072] [arXiv:1501.04964] [INSPIRE].

[28] H.A. Weldon, *Simple Rules for Discontinuities in Finite Temperature Field Theory*, *Phys. Rev.* **D 28** (1983) 2007 [INSPIRE].

[29] M. Laine, *Thermal 2-loop master spectral function at finite momentum*, *JHEP* **05** (2013) 083 [arXiv:1304.0202] [INSPIRE].

[30] P. Hernández, M. Kekic, J. López-Pavón, J. Racker and J. Salvado, *Testable Baryogenesis in Seesaw Models*, *JHEP* **08** (2016) 157 [arXiv:1606.06719] [INSPIRE].

[31] J. Ghiglieri and M. Laine, *GeV-scale hot sterile neutrino oscillations: a numerical solution*, *JHEP* **02** (2018) 078 [arXiv:1711.08469] [INSPIRE].

[32] K. Kamada and A.J. Long, *Baryogenesis from decaying magnetic helicity*, *Phys. Rev.* **D 94** (2016) 063501 [arXiv:1606.08891] [INSPIRE].

[33] A.J. Long, E. Sabancilar and T. Vachaspati, *Leptogenesis and Primordial Magnetic Fields*, *JCAP* **02** (2014) 036 [arXiv:1309.2315] [INSPIRE].

[34] D.T. Son and P. Surowka, *Hydrodynamics with Triangle Anomalies*, *Phys. Rev. Lett.* **103** (2009) 191601 [arXiv:0906.5044] [INSPIRE].

[35] P.B. Arnold, G.D. Moore and L.G. Yaffe, *Transport coefficients in high temperature gauge theories. 1. Leading log results*, *JHEP* **11** (2000) 001 [hep-ph/0010177] [INSPIRE].